Contrasting Features of Papillary and Chromophobe Renal Cell Carcinoma Revealed by Whole-Genome Sequencing

Richard Culliford[1], Charlie Mills[1], Daniel Chubb[1], Ben Kinnersley[1,2], Amit Sud[1], Alex J. Cornish[1], Lisa Browning[3], Samuel E.D. Lawrence[1], Robert Bentham[2], Anna Frangou[4,5], Andreas J. Gruber[6], Kevin Litchfield[7], David C. Wedge[8,9], James Larkin[10,11], Samra Turajlic[10,11,12], and Richard S. Houlston[1]

ABSTRACT

The identification of cancer drivers is a cornerstone to the delivery of precision oncology. So far, sequencing of renal cell cancer (RCC) has largely been confined to the clear cell subtype of RCC. In contrast, sequencing analyses of the less common forms of RCC, papillary RCC (pRCC) and chromophobe RCC (ChRCC), have so far been limited. We analyzed whole-genome sequencing data on 164 tumor–normal pairs from the Genomics England 100,000 Genomes Project, providing a comprehensive, high-resolution map of copy number alterations, structural variation, and key global genomic features, including mutational signatures, intratumor heterogeneity, and analysis of extrachromosomal DNA formation. Our research establishes correlations between genomic alterations and histologic diversification and the extent to which genetically-mediated immune escape contributes to the development of these RCC subtypes.

Implications: We demonstrate the distinctive genetics that characterizes pRCC and ChRCC and how this information has the potential to inform patient treatment and clinical trials.

Introduction

Most kidney cancers are renal cell carcinomas (RCC). The World Health Organization (WHO; fifth edition) classification of RCC recognizes more than 20 subtypes (1), with 70% to 90% having clear cell histology (ccRCC). There has been significant progress in the treatment of ccRCC over the past 20 years (2). In contrast, less progress has been made in the treatment of papillary RCC (pRCC) and chromophobe RCC (ChRCC), which account for 13% to 20% and 5% to 7% of RCC cases, respectively (3).

The need to understand cancer biology and etiology, inform the development of novel therapies, and better predict patient outcomes has been a motivation in sequencing studies of cancer. So far, these studies of RCC have largely been confined to ccRCC (4–6), and studies of pRCC and ChRCC have generally been limited to exome sequencing of small numbers of cases (7). To address this shortcoming, we report the analysis of whole-genome sequencing (WGS) data generated on tumor–normal (T/N) pairs from 164 patients recruited from NHS Genomic Medicine Centres (GMC) across England, as part of the Genomics England 100,000 Genomes Project (100kGP, RRID: SCR_010502; refs 8, 9). Our study provides an extensive analysis of the genomic landscape, mutational processes, and clonal architecture underlying the development of ChRCC and pRCC.

Materials and Methods

Patients and ethics

The cohort (100kGP, release version 14) comprised T/N sample pairs with primary ChRCC and pRCC recruited through 13 GMCs. The study was conducted as part of the 100kGP, approved by the East of England-Cambridge South Research Ethics Committee (reference: 14/EE/1112), with all patients providing written informed consent. Patients were routine surgical cases, and tumor pathology was reported by diagnostic histopathologists at contributing centers. Histology of tumors was initially as per WHO fourth edition (10) but was updated herein to WHO fifth edition (1). DNA, extracted from EDTA-venous blood samples, served as a source of the patient germline. To avoid sequencing bias associated with polymerase chain reaction (PCR) amplification, we restricted our analysis to WGS data generated from PCR-free, fresh-frozen tumors from 103 patients with pRCC (67 male; median age 62, range 37–87) and 61 patients with ChRCC (24 male; median age 62, range 26–83; Supplementary Tables S1 and S2). We subdivided ChRCC cases into "eosinophilic" ($n = 13$) and "classical" ($n = 48$; Supplementary Table S2). Cognizant of the emerging molecular subtypes of RCC, we sought evidence of *TSC1/TSC2* mutations in eosinophilic cases or SDH alterations, which would justify reclassification as eosinophilic solid and cystic RCC or SDH-deficient RCC, respectively. No

[1]Division of Genetics and Epidemiology, The Institute of Cancer Research, London, United Kingdom. [2]Department of Oncology, University College London Cancer Institute, London, United Kingdom. [3]Department of Cellular Pathology, Oxford University Hospitals NHS Foundation Trust, Oxford, United Kingdom. [4]Algebraic Systems Biology, Max Planck Institute of Molecular Cell Biology and Genetics, Dresden, Germany. [5]Algebraic Systems Biology, Centre for Systems Biology Dresden, Dresden, Germany. [6]Department of Biology, University of Konstanz, Konstanz, Germany. [7]The Tumour Immunogenomics and Immunosurveillance Lab, University College London Cancer Institute, London, United Kingdom. [8]Manchester Cancer Research Centre, University of Manchester, Manchester, UK. [9]NIHR Manchester Biomedical Research Centre, Manchester, United Kingdom. [10]Renal and Skin Units, The Royal Marsden NHS Foundation Trust, London, United Kingdom. [11]Melanoma and Kidney Cancer Team, The Institute of Cancer Research, London, United Kingdom. [12]Cancer Dynamics Laboratory, The Francis Crick Institute, London, United Kingdom.

R. Culliford and C. Mills contributed equally to this article.

Corresponding Author: Richard Culliford, Division of Genetics and Epidemiology, The Institute of Cancer Research, 123 Old Brompton Road, London SW7 3RP, United Kingdom. E-mail: richard.culliford@icr.ac.uk

Mol Cancer Res 2026;XX:XX–XX

doi: 10.1158/1541-7786.MCR-25-0616

TSC mutations were detected in any of the eosinophilic cases, and although one ChRCC was shown to have an *SDHA* somatic mutation, this was predicted to be benign (Supplementary Methods S1), thereby precluding tumor reclassification (11).

WGS

Illumina Inc. conducted 150 base pair (bp) paired-end WGS using HiSeq X technology. Germline and tumor samples were sequenced to an average depth of 30× and 100×, respectively. Tumor purity and ploidy were estimated as per Van Loo and colleagues (12), as part of a pipeline incorporating Battenberg (RRID:SCR_017098, version 2.2.8; ref. 13) for copy number (CN) alteration calling and whole-genome duplication (WGD) in tumor samples (Supplementary Methods S1). The median tumor purity was 0.79 (range 0.21–0.97) and 0.74 (0.20–0.98) for ChRCC and pRCC, respectively (Supplementary Table S2). Further details on sample curation, tumor purity, and WGS are provided in Supplementary Methods S1.

Statistical analysis

We used IntOGen (RRID: SCR_027727; ref. 14) to identify coding drivers (Supplementary Methods S1). We searched for noncoding drivers in core promoters, distal promoters, untranslated regions, and splice regions using OncodriveFML (RRID: SCR_027731; ref. 15) and ActiveDriverWGS (RRID: SCR_027737; ref. 16). Positive or negative selection of mitochondria (mt) mutations in 12 mt protein-coding genes (excluding *MT-ND6* due to strand bias) was inferred using dNdScv (RRID: SCR_017093; ref. 17). Pathways containing driver genes were referenced to PubMed and interrogated using ActivePathways (RRID: SCR_027736; ref. 18) and MSigDB (RRID: SCR_016863, version 7.5.1; ref. 19). The evolutionary timings of driver mutations were estimated using MutationTimeR (RRID: SCR_027739, v0.99.3; ref. 20) and ordered using a league model approach, whereby multinomial distributions describing the expected ordering of pairs of driver mutations are repeatedly sampled to generate the ordering of mutations (Supplementary Methods S1).

Recurrent arm-level CN events, focal amplifications, and focal deletions were identified using GISTIC (RRID: SCR_000151, version 2.0.2.3; ref. 21; Supplementary Figs. S1 and S2; Supplementary Table S3). Structural variants (SV) were identified from a consensus of three SV calling algorithms and classified as simple or complex using ClusterSV (RRID: SCR_027722; ref. 22) with hotspots assigned as per Glodzik and colleagues (Supplementary Fig. S3; Supplementary Methods S1; ref. 23). Amplicon structures were identified using AmpliconArchitect (RRID: SCR_023150; ref. 24). Telomere length of germline and tumor DNA was estimated from their respective bam files using Telomerecat (RRID: SCR_027747, version 3.3.0; ref. 25), adopting default parameters.

De novo extraction of single-base substitution (SBS) and insertion and deletion (ID) mutational signatures, including decomposition to known COSMIC signatures (RRID: SCR_002260, version 3.2; ref. 26), was performed using SigProfilerExtractor (RRID: SCR_023121, version 1.1.4; ref. 27). We used mSINGS (RRID: SCR_027728; ref. 28) and HRDetect (RRID: SCR_027726; ref. 29) to identify mismatch repair deficient (dMMR) and homologous recombination deficient (dHR) tumors.

Genomes were HLA-typed using POLYSOLVER (RRID: SCR_022278; ref. 30), and neoantigens were predicted using pVAC-Seq (RRID: SCR_025435, v3.1.2; ref. 31). We considered tumors as having genetically predicted immune escape on the basis of a nonsynonymous mutation or loss of heterozygosity (LOH) in any HLA class I gene or an inactivating mutation in one of 22 antigen-presenting genes (APG). T-cell ExTRECT (RRID: SCR_027742; ref. 32) was used to estimate the T-cell receptor-α chain T-cell fraction within tumor samples from WGS, which was used as a proxy measurement of T-cell infiltration. Further details of bioinformatic analyses are provided in Supplementary Methods S1.

To compare frequencies of categorical variables with molecular features, we used Fisher's exact test or logistic regression. For quantitative traits, we used *t* tests, Wilcoxon rank-sum test, linear regression, or negative binomial regression. In all cases, we considered a two-sided P value < 0.05 as being statistically significant.

Results

None of the patients were carriers of a pRCC (i.e., *MET*, *PTEN*, *FH*) or ChRCC susceptibility gene (i.e., *TSC1*, *TSC2*, *PTEN*, or *FLCN*; Supplementary Table S5; ref. 33). As previously documented (7), ChRCCs displayed a low tumor mutational burden (TMB) [median 0.61/Mb, median ploidy 1.7, and weighted genome instability index (WGII) 34.8%]. In contrast, pRCC was characterized by a higher TMB (1.79/Mb, ploidy 2.19, WGII of 22.6%), similar to ccRCC (6). Germline samples tended to have a longer telomere compared with their matched tumor in both the ChRCC (mean germline TL = 4,700, mean tumor TL = 4,151, *t* test $P = 0.02$) and pRCC (mean germline TL = 4,567, mean tumor TL = 3,542, *t* test $P = 2.19 \times 10^{-14}$) cohorts as expected. There was no significant difference in the mean germline–tumor telomere difference between eosinophilic and classical ChRCC (eosinophilic ChRCC mean telomere difference = −700, classical ChRCC mean telomere difference = −509, *t* test $P = 0.76$; Supplementary Fig. S4; Supplementary Table S2).

Structural alterations

ChRCC and pRCC tumors showed distinctive chromosomal profiles— markedly different from ccRCC (**Fig. 1**; Supplementary Tables S6 and S7; refs. 4, 6). As previously reported (7, 11, 34), most classical ChRCCs showed loss of chromosomes 1, 2, 6, 10, 13, 17, and 21, in contrast to the eosinophilic cases (Supplementary Figs. S5A and S5B, S6A and S6B). In comparison, pRCCs showed gain of chromosome 7 and/or 17 (76%, 78/103), accompanied by gain of chromosomes 3, 12, 16, and 20, albeit at a lower frequency (**Fig. 1**; Supplementary Table S6).

WGD was identified in 20% (12/61) of ChRCC tumors, similar to ccRCC (6), but only 5% (5/103) of pRCC. Eosinophilic ChRCC tumors were also likely to have WGD detected in comparison with their noneosinophilic counterparts (1/13 vs. 11/48). In contrast to many other cancer types, such as breast and colorectal (35), WGD in ChRCC was not associated with *TP53* mutations (Fisher's exact test, $P = 1.0$), with only 21% (3/14) of *TP53*-mutated tumors also being positive for WGD (Supplementary Table S2).

We identified three SV hotspot regions in ChRCC tumors (Supplementary Table S8; Supplementary Fig. S8A–S8C), one defined by chr5:12448-1417975, which encompassed *TERT* and *SDHA*, in five tumors. None harbored a coding change in *TERT*. However, a missense mutation in *SDHA* was detected in one cancer. No SV hotspot regions were identified in pRCC tumors. ecDNA has been associated with oncogene amplification and poor outcomes in some cancers. Complex rearrangements were identified in 5% (3/61) of ChRCC and 16% (17/103) of pRCC, implicating *CDK6*. However, in contrast to many cancers (36), ecDNA was not a common feature of either RCC subtype, only being identified in 3% (2/61) of ChRCC and 7% (7/103) of pRCC (Supplementary Fig. S9).

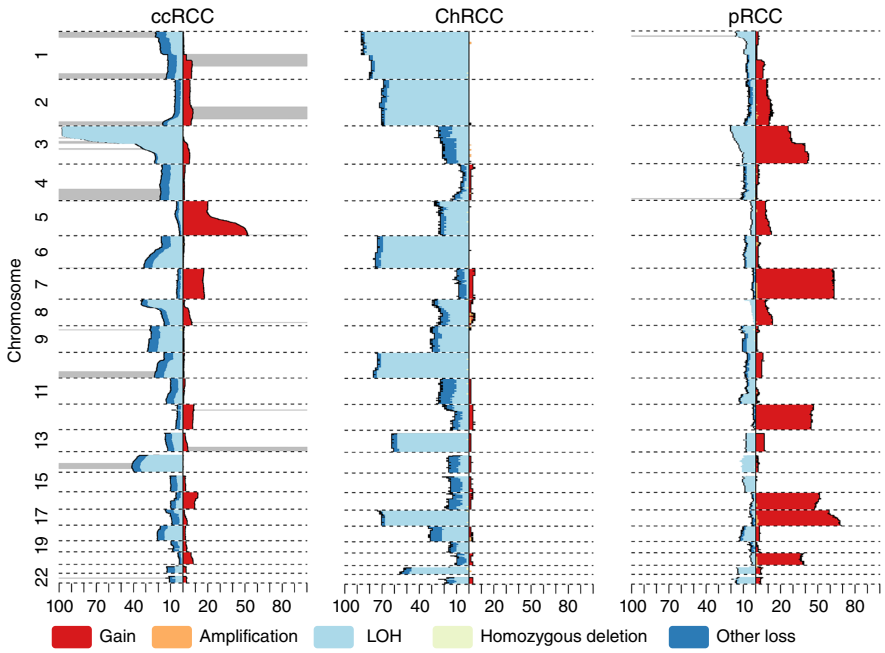

Figure 1.
Contrasting copy-number profiles of ccRCC, ChRCC, and pRCC. Information on ccRCC copy number from Culliford and colleagues (6).

Cancer drivers

We identified seven genes significantly mutated in ChRCC (*BAP1*, *CDKN1A*, *CSPG4*, *MAP3K13*, *MTOR*, *TP53*, and *WNK2*) and 14 genes in pRCC (*ARID1A*, *CACNA1D*, *ELF3*, *KDM5A*, *KIAA1549*, *KMT2C*, *LEPROTL1*, *MAP3K1*, *MET*, *MTOR*, *NFIB*, *PBRM1*, *SETD2*, and *UBR5*). None of these drivers were associated with recurrent hotspot mutations, and mutational frequencies were broadly concordant with published data (Supplementary Fig. S10A and S10B; Supplementary Tables S9 and S10). In our analysis, there was no evidence for mutual exclusivity in any of these driver genes (Fisher's exact test, $P < 0.05$).

We conducted a further search under a restricted hypothesis by considering genes previously implicated in RCC (14, 37, 38). This analysis provided additional support for the role of 12 genes in ChRCC (*ATM*, *CDKN2A*, *FLT4*, *GRM3*, *KMT2D*, *NRAS*, *PTEN*, *RB1*, *SDHA*, *TSC1*, *TSC2*, and *UBR5*) and eight genes in pRCC (*BAP1*, *FAT1*, *KDM6A*, *NF2*, *NFE2L2*, *SMARCB1*, *STAG2*, and *TP53*; **Fig. 2** and **3**; Supplementary Table S10). Extending our analysis to consider genes implicated by virtue of focal genomic alterations provided additional support for *ARID1A* in pRCC (Supplementary Table S7).

Considering large-scale chromosomal alterations provided support for reported drivers in ChRCC and pRCC (Supplementary Figs. S11 and S12; Supplementary Tables S6, S9, and S10). *CDKN1A* (del6p21.2), *PTEN* (del10q23.31), *RB1* (del13q4.2) and *TP53* (del17p13.1) are supported as drivers in ChRCC. In contrast to previous reports (37), our analysis did not provide evidence to implicate *TSC1* and *TSC2* in either classical or eosinophilic ChRCC. In pRCC, alterations implicated *KDM5A* (amp12p13.33), *KIAA1549* (amp7q34), and *MET* (amp7q31.2). In our analysis, there was no evidence to support any driver gene in ecDNA.

Searching for noncoding drivers identified the core promoter region of *TERT* as recurrently mutated in 11 pRCC tumors, 10 of which harbored the rs1242535815 mutation, which has been documented to be disease-causing in RCC and other tumor types (Supplementary Table S11; refs. 39–41). The difference in TL between tumor and germline was significantly larger in tumors harboring *TERT*-promoter mutations (tumor–germline TL difference: -1700 for mutated and -945 for wild-type, *t* test $P = 0.0068$). Presumptive pathogenic mutations identified the *CCDC107* distal promoter region as a driver in pRCC.

Our analysis emphasizes the differences in gene pathways between the RCC subtypes (42), specifically the importance of mutations in the PI3K/AKT/mTOR and p53/p21/RB1 pathways in ChRCC (**Fig. 4**; Supplementary Fig. S13). There was limited evidence to support the mutation of chromatin modifier genes in the development of ChRCC, in contrast to pRCC or ccRCC (6). The mutation of *MET* was essentially confined to pRCC. In terms of clonal architecture, *MTOR* and *TP53*-related genes were early mutational events in the development of ChRCC. Similarly, the mutation of *PBRM1* was an early event in the pRCC tumors. In contrast, *ELF3* mutations in pRCC tumors tended to be a late event (Supplementary Fig. S14).

Mitochondrial DNA analysis

There is increasing evidence for mt dysregulation in cancer (43). Although mitochondrial DNA mutation rates were not significantly different between ChRCC (including eosinophilic) and pRCC, the frequency of mtCN was significantly higher in pRCC tumors (*t* test, $P < 0.001$; Supplementary Fig. S15A and S15B; Supplementary Tables S2 and S12).

Across histologies, we identified mutated genes in complexes I and III under positive selection and genes in complex IV, which were typically negatively selected. Irrespective of heteroplasmy, *MT-CYB* showed evidence of being under positive selection for missense mutations in ChRCC (dN/dS = 1.84, $P = 0.03$). *MT-ND2* showed a higher proportion of high VAF missense mutations in pRCC (dN/dS = 4.91, $P = 0.0048$). Although *MT-ND4* was positively selected in ChRCC for low VAF missense mutations (dN/dS = 1.94, $P = 0.02$), there was no evidence that ChRCC tumors were more likely to be *MT-ND4*–positive (Fisher's exact test $P = 1$) or *MT-ND5*–positive (Fisher's exact test $P = 1.0$) than pRCC tumors (Supplementary Tables S13 and S14).

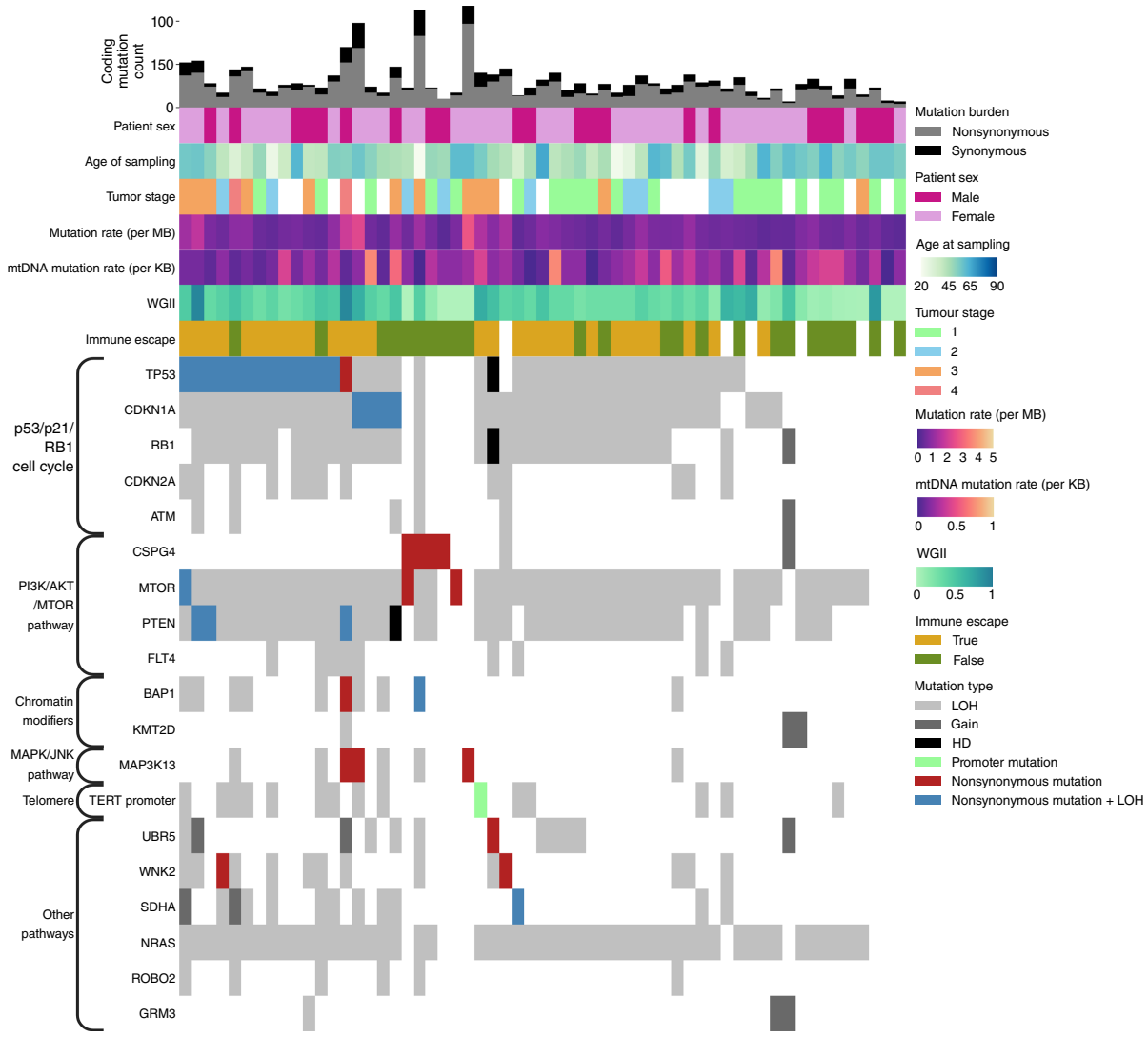

Figure 2.
Relationship between genomic profile and clinical features for ChRCC ($n = 59$). Samples are ordered by the highest coding mutational burden for each histology. Genes are ordered by major pathways, followed by mutation status and then copy number alteration. HD, homozygous deletion; KB, kilobase; LoH, loss of heterozygosity; MB, megabase; mtDNA, mitochondrial DNA; WGII, weighted genome instability index.

Mutational signatures

To gain insight into mutational processes, we extracted decomposed COSMIC SBS and ID mutational signatures (RRID:SCR_002260, version 3.2) for each tumor (**Fig. 5A** and **B**; Supplementary Fig. S15; Supplementary Table S15). In both tumor types, SBS1 and SBS5, resulting from clock-like mutagenic processes, were ubiquitous. One hypermutated ChRCC tumor with the *POLE* and *POLD1* mutations (Supplementary Table S5; Supplementary Fig. S13) displayed SBS26 and SBS44, reflective of dMMR. ID1 and ID2, a consequence of replication slippage, were frequent in ChRCC, with a lower presence of ID12 (unknown etiology). The same ID signatures were also a feature of pRCC, albeit ID1 was at a higher frequency compared with ChRCC (99% vs. 86.9%), whereas ID2 (76.7% vs. 93.4%) and ID12 (5.8% vs. 32.8%) showed lower frequencies (**Fig. 5A** and **B**; Supplementary Fig. S14; Supplementary Table S15). None of the tumors showed evidence of dHR.

Immune evasion

We predicted 2,051 class I neoantigens across 55 ChRCC ($n = 867$, 0–607/tumor, median 1) and 86 pRCC ($n = 1184$, 0–65/tumor, median 9) tumors; >95% were a consequence of frameshift variants. There was no difference in the distribution of neoantigen counts between eosinophilic and classical ChRCC tumors (Wilcoxon rank-sum $P = 0.42$). We detected LOH of HLA in 48% ($n = 29$) of ChRCC and 4% ($n = 3$) of pRCC tumors. There was no association between indel burden and HLA allele status in ChRCC or pRCC, and no tumors had HLA mutations. Only one ChRCC harbored an APG mutation, whereas no pRCC tumors had APG mutations. Collectively, these data showed that 49% of ChRCC had evidence of genetically predicted immune evasion (albeit primarily a consequence of chromosome 6 loss), but this was only a feature of 4% of pRCCs. There was a positive correlation between the mutation of *TP53* and genetically predicted

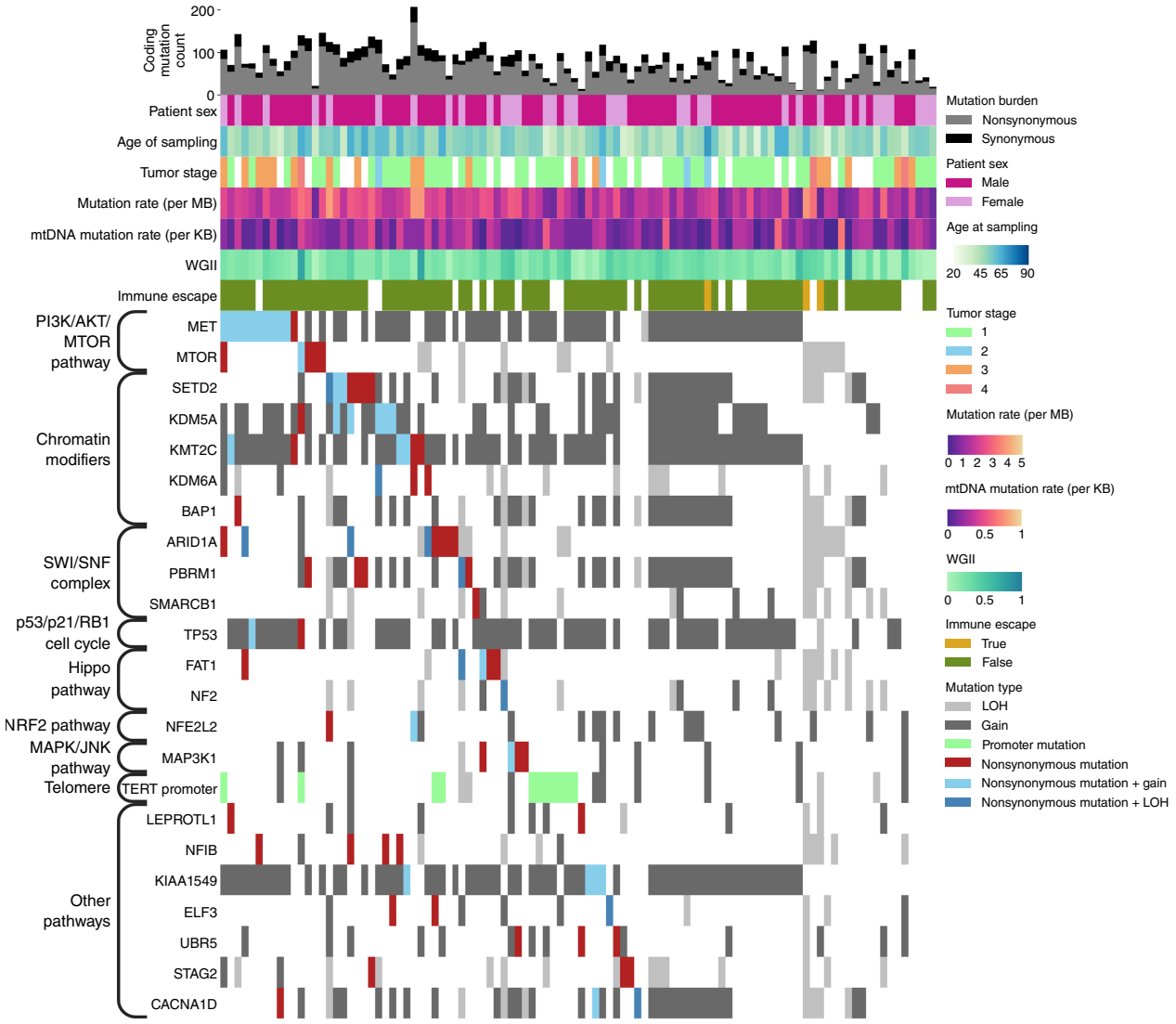

Figure 3.

Relationship between genomic profile and clinical features for pRCC ($n = 102$). Samples ordered by highest coding mutational burden for each histology. Genes are ordered by major pathways, followed by mutation status and then copy-number alteration. KB, kilobase; LoH, loss of heterozygosity; MB, megabase; mtDNA, mitochondrial DNA; WGII, weighted genome instability index;.

immune escape (OR = 7.4, Fisher's exact test, $P = 0.01$) in ChRCC.

Clinicopathologic relationships

In both ChRCC and pRCC, age at sampling was correlated with TMB (univariate linear regression $P = 0.04$) and SV burden (univariate negative binomial regression $P = 0.01$), whereas stage was positively associated with chromosomal aberrations (Fisher's exact test $P = 0.01$). SV burden and T-cell infiltration were positively associated with higher grade in pRCC (univariate linear regression $P = 4.0 \times 10^{-12}$ and Fisher's exact test $P = 0.04$, respectively). Furthermore, higher-stage ChRCC and pRCC tumors were more likely to have *TP53* (Fisher's exact test $P = 0.02$) and *MET* mutations (Fisher's exact test $P = 0.014$), respectively.

Increased mtCN was associated with WGD in ChRCC tumors (multivariate linear regression, $P = 6.49 \times 10^{-12}$). Across all tumors, T-cell infiltration was not associated with neoantigen burden, but an increased number of heterozygous HLA-I allele pairs was associated with increased infiltration in ChRCC (multivariate logistic regression $P = 0.04$). ChRCC tumors that showed evidence of LoH-induced immune escape were more likely to be *TP53*-mutated (multivariate logistic regression $P = 0.04$), a feature irrespective of neoantigen burden (**Fig. 6A** and **B**; Supplementary Tables S16–S20).

Clinical actionability of genomic features

We assessed the actionability of driver genes by referencing OncoKB (RRID: SCR_014782, version 3.11; ref. 44). For ChRCC and pRCC, we identified 1 and 2 unique OncoKB annotated

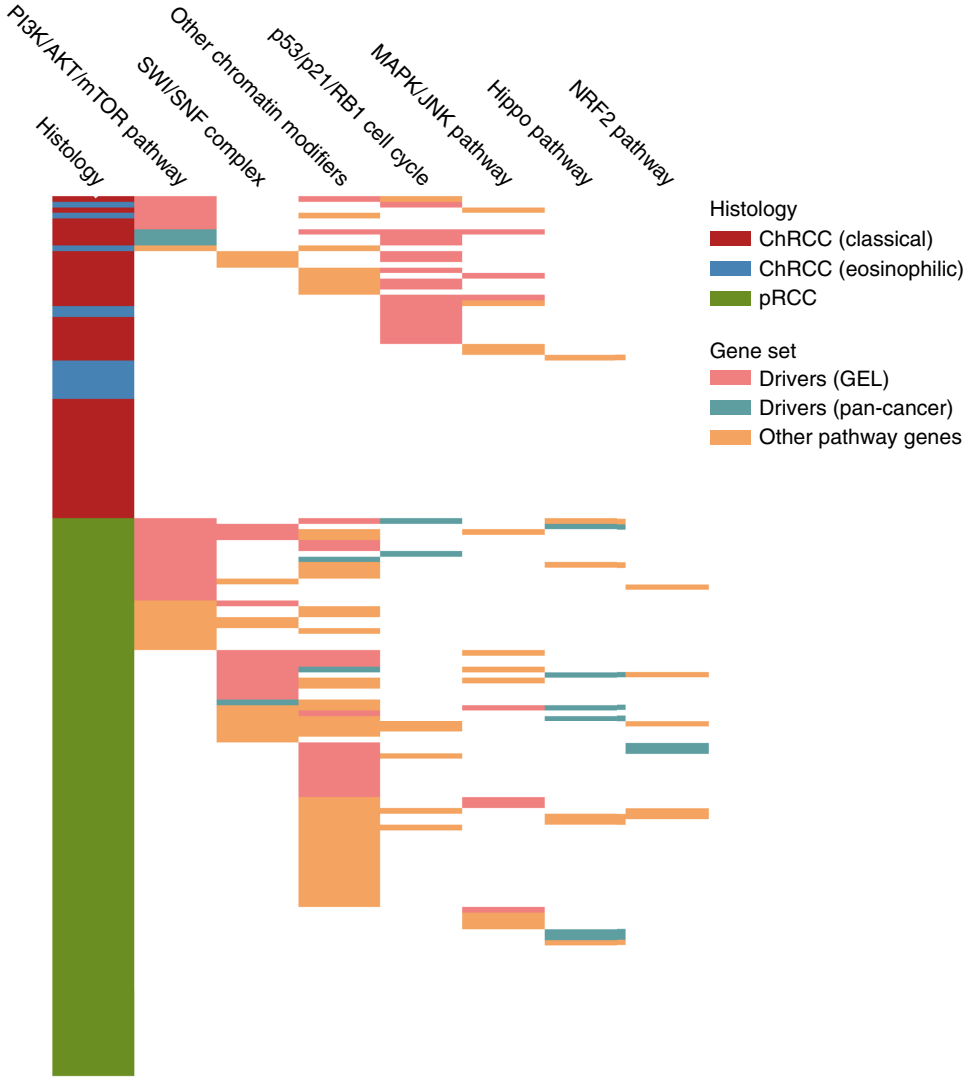

Figure 4.
Major biological pathways disrupted in ChRCC (n = 59) and pRCC (n = 102). Genes in "pan-cancer" refer to driver genes that are recurrently mutated in Bailey and colleagues (42). Genes in "other pathway genes" refer to all other canonical genes, including noncancer driver genes, within the corresponding cellular pathway (Supplementary Methods S1). GEL, Genomics England 100,000 Genomes Project.

alterations, respectively, in *MTOR* that were targetable (level 3a–4). This included L2427Q identified in one ChRCC and one pRCC, which has clinical evidence (level 3b) in RCC of being targetable by temsirolimus. Standard-of-care treatment of amplified *MET*-positive non–small cell lung cancer suggests that 63% (65/103) of *MET*-amplified positive pRCC might be eligible for capmatinib, crizotinib, or tenpotinib. In pRCC, there was level 4 evidence that inactivating mutations in *ARID1A* could be targetable with PLX2853 or tazemetostat. To complement this analysis, we first examined the COSMIC Mutation Actionability in Precision Oncology database (RRID:SCR_002260; ref. 26), highlighting an additional 30 unique mutations as potentially targetable. Notably there are ongoing early-phase trials targeting *MET* in pRCC, based on cabozantinib and savolitinib, and PF-04217903 targeting M1250T. Additionally, solid tumors with *ARID1A*, *BAP1*, and *MTOR* mutations are the subject of ongoing trials (Supplementary Table S21). To broaden our search for novel therapeutic avenues, we examined whether any of the RCC driver genes might be candidates for synthetic lethality using SYLVER (RRID:SCR_027764, ref. 45), identifying that *PBRM1* deficiency may be amenable to receptor tyrosine kinase inhibition.

Discussion

We have sought to advance our understanding of non-ccRCC subtypes by analyzing WGS data from ChRCC and pRCC tumors. Our analysis emphasizes the very distinctive genomic profile of these RCC tumor subtypes. As well as confirming established drivers, we further highlight p53/p21/RB1 (G_1/S) cell cycle, PI3K/AKT/mTOR, and chromatin modifier pathways as being central to the biology of ChRCC. In comparison, *MET* and chromatin modifiers were a central feature of pRCC. Furthermore, our analysis validates previous reports of structural abnormalities associated with these non-ccRCC tumors. We did not confirm the reported very high rate of WGD in ChRCC of 60%; however, this previous work was based on an analysis of only 10 tumors (46). In contrast to our ccRCC signature analysis (6), this study did not provide support to implicate either tobacco smoking or exposure to aristolochic acid as a risk factor for either ChRCC or pRCC.

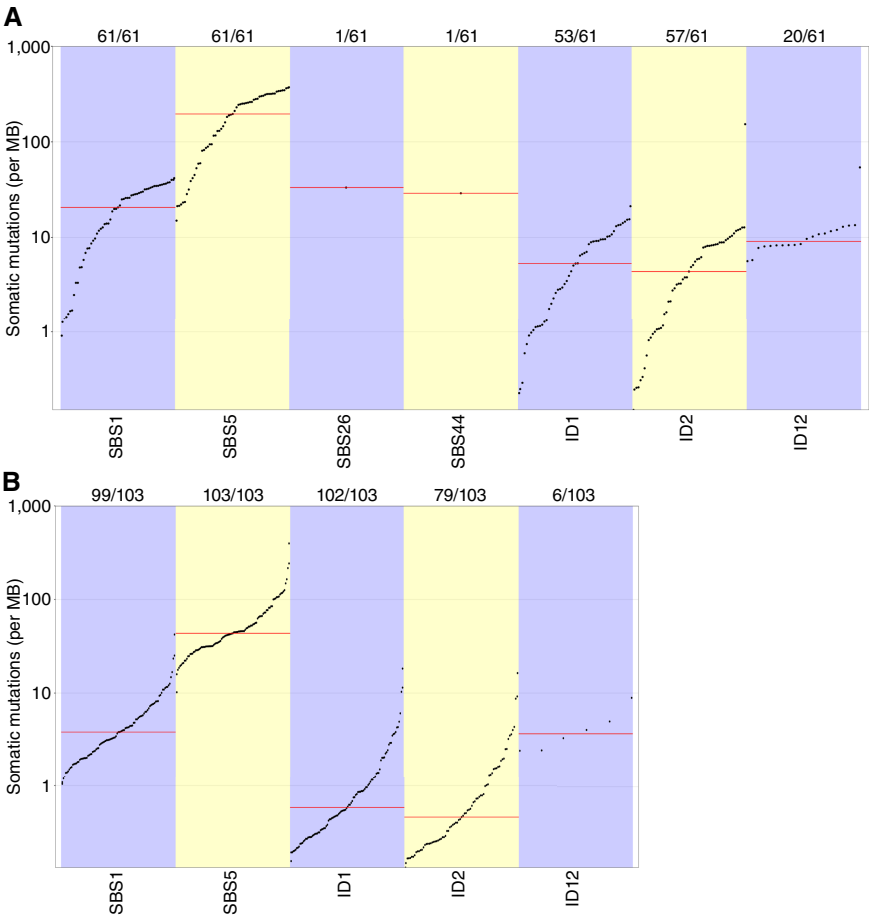

Figure 5.

Mutation rate associated with each COSMIC signature. **A,** ChRCC ($n = 61$) and (**B**) pRCC ($n = 103$). ID1, slippage during DNA replication of the replicated DNA strand; ID2, slippage during DNA replication of the replicated DNA strand; ID12, unknown etiology; MB, megabase; SBS1, spontaneous deamination of 5-methylcytosine (clock-like signature); SBS5, unknown (clock-like signature); SBS26, defective DNA mismatch repair; SBS44, defective DNA mismatch repair.

Our observations reinforce the desirability of subtype-specific treatment paradigms for non-ccRCC. To investigate the prospect of targeting specific driver mutations, we queried OncoKB, which is regularly curated by an expert panel and is therefore generally considered to reflect the current state of knowledge. As other investigators have reported a higher targetable variant detection rate by applying multiple tools to annotate variants, we also made use of the COSMIC resource. Most of the alterations we describe as being actionable are based on clinical evidence from other cancers or biological plausibility. As per previous reports, most of the targetable alterations we identified are within PI3K/mTOR pathway genes. Although the mTOR inhibitors temsirolimus and everolimus have received regulatory agency approval, their clinical benefit in non-ccRCC tumors is modest (47).

Although the management of ccRCC has been transformed by immune checkpoint inhibitors (ICI), a recent review of ICI clinical trials has concluded that only 6% of ChRCC respond to ICIs (48). Although one of the ChRCC cases had a hypermutated phenotype and thus might be amenable to ICI, in our analysis, most ChRCCs were immunologically cold, showing a low mutational rate, high HLA loss, and limited T-cell infiltration. Moreover, our analysis of ChRCC aligns with previous reports of *TP53*-mediated immune evasion as a general feature of cancer (49). Recent data from phase II trial studies suggest that ICIs such as ipilimumab/nivolumab may hold promise as first-line treatment for patients with metastatic non-ccRCC cancers (50, 51). Notably, in the case of pRCC, the lack of genetically predicted immune escape may underpin the observation that patients treated with ICI have been reported to have a better outcome than patients solely receiving a tyrosine kinase inhibitor (TKI) as first-line therapy (51).

Because of its low incidence, the treatment for non-ccRCC has largely been based on evidence from small phase II clinical trials or extrapolated from successful therapies in ccRCC. Nevertheless, several phase II trials have shown the promise of MET inhibitors in the management of metastatic pRCC, demonstrating superior clinical activity compared with conventional TKIs and leading to less reliance on solely targeting the PI3K axis (Supplementary Table S21). An important caveat to our analysis is that the genetic profiles we derived are from a single region, which has potentially limited our ability to detect clinically important subclonal targetable alterations.

In many other cancers, a high mutational and neoantigen burden has been linked to better overall survival and responsiveness to checkpoint inhibitors, presumably reflecting native immune responsiveness. Conversely, immune escape of tumors by virtue of HLA loss or mutation of APGs has been linked to worse clinical outcomes. Given that immune escape was a more common feature of ChRCC, this may explain the poorer clinical response of metastatic ChRCC tumors compared with pRCC and other non-ccRCC

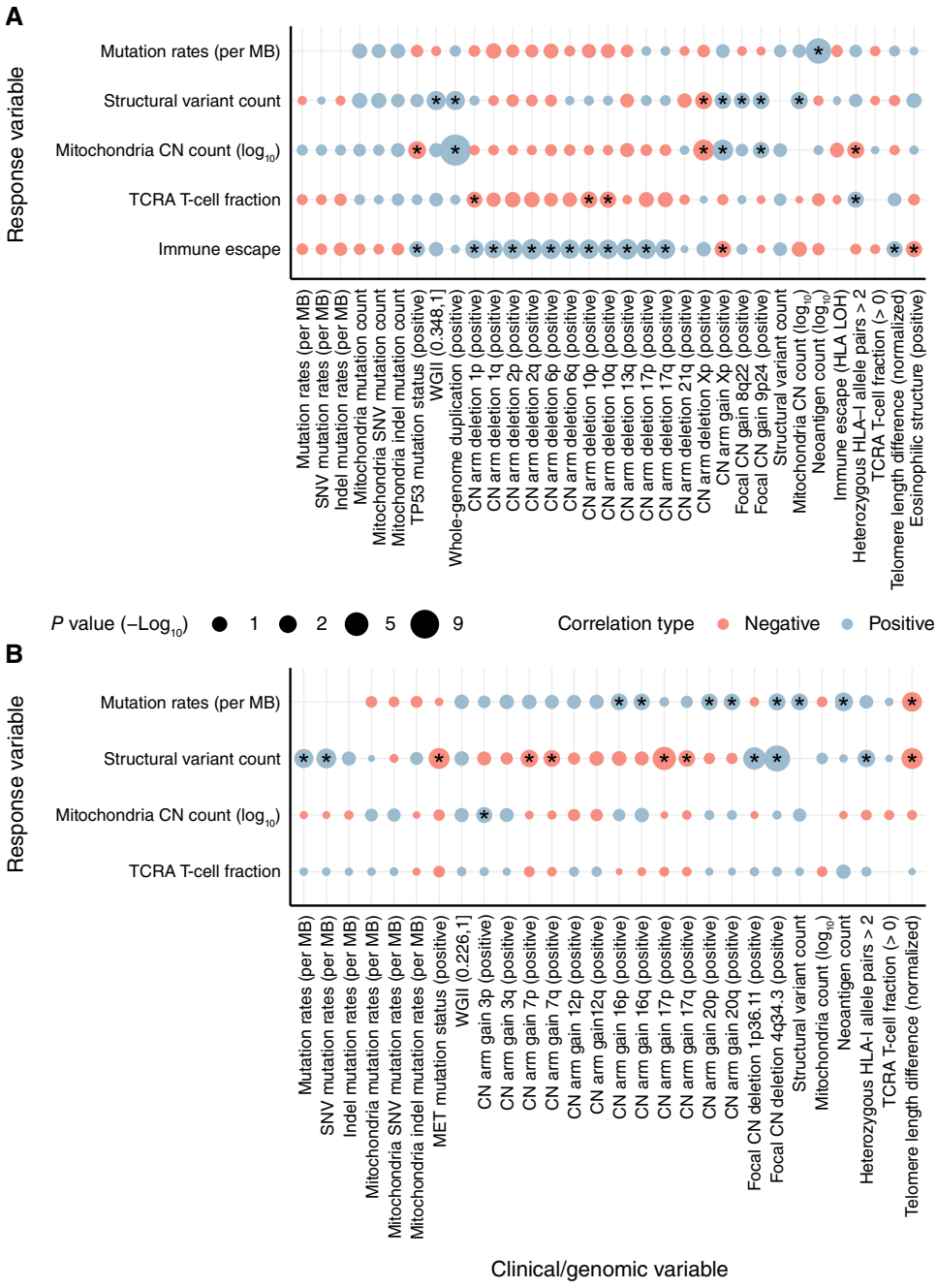

Figure 6.

Summary of clinical correlations adjusted for sex, age of sampling, and stage. **A,** ChCC (n = 61) and (**B**) pRCC (n = 103). CN, copy number; MB, megabase; SNV, single-nucleotide variant; TCRA, T-cell receptor-α; WGII, whole-genome instability index; *, $P < 0.05$.

tumors to PD-1 inhibitors in retrospective analyses or clinical trials (i.e., pembrolizumab in the KEYNOTE 427-b study; refs. 52, 53).

In conclusion, our observations reinforce calls that the distinctive genetics associated with subtypes of RCC tumors has potential value in informing the design of clinical trials of RCC (54).

Data Availability

The data analyzed in this study are available from Genomics England Ltd. Restrictions apply to the availability of these data, which were used under license for this study. The data were deposited in the National Genomic Research Library and can be accessed via the Genomics England Research Environment secure cloud workspace. Access can be obtained by first applying to become a member of either the Genomics England Research Network (https://www.genomicsengland.co.uk/research/academic) or the Discovery Forum (industry partners https://www.genomicsengland.co.uk/research/research-environment). The process for joining the network is described at https://www.genomicsengland.co.uk/research/academic/join-gecip and consists of the following steps:

1. Your institution will need to sign a participation agreement available at https://files.genomicsengland.co.uk/documents/Genomics-England-GeCIP-Participation-Agreement-v2.0.pdf and email the signed version to gecip-help@genomicsengland.co.uk.
2. Once you have confirmed your institution is registered and have found a domain of interest, you can apply through the online form at https://www.genomicsengland.co.uk/research/academic/join-gecip, in which you can

specify the reason for access and the expected timeframe for which you wish to have access. Once your Research Portal account is created, you will be able to log in and track your application.
3. Your application will be reviewed within 10 working days.
4. Your institution will validate your affiliation.
5. You will need to complete the online information governance training and will be granted access to the research environment within 2 days of passing the online training.

The processed clinical and genomic data applied to the investigation are available in the Research Environment within the folder /re_gecip/shared_allGeCIPs/rculliford/RCC_landscape. At present, there is no proposed end date for data access within the research environment. All other public/private datasets used in the study, including corresponding download links and version numbers, can be found in Supplementary Table S4.

After completion of the instructions given by the Data Availability statement, code to allow for reproducibility of results and figures is available in the research environment within the folder /re_gecip/shared_allGeCIPs/rculliford/RCC_landscape. Sources of each software package and externally downloaded data are detailed in Supplementary Table S4.

Authors' Disclosures

L. Browning reports other support from the National Institute for Health Research (NIHR) Oxford Biomedical Research Centre during the conduct of the study. A.J. Gruber reports grants from DFG, HBS, AFF, and BIS outside the submitted work. K. Litchfield reports other support from Isomorphic Labs outside the submitted work. J. Larkin reports personal fees from Eisai, Incyte, Merck, touchIME, touchEXPERTS, GSK, iOnctura, Dynavax, CRUK, Apple Tree, Boston Biomedical, YKT Global, Pierre Fabre, EUSA Pharma, AstraZeneca, Aptitude, Calithera, Ultimovacs, Seagen, eCancer, Ervaxx, and Iovance; grants and personal fees from Novartis, Pfizer, Roche, Bristol Myers Squibb, MSD, and Immunocore; and grants from Achilles Therapeutics, Nektar Therapeutics, Covance, Pharmacyclics, Aveo, and NIHR Royal Marsden Institute of Cancer Research Biomedical Research Centre during the conduct of the study. S. Turajlic reports grants from Cancer Research UK, The Francis Crick Institute, the Wellcome Trust, NIHR Biomedical Research Centre at the Royal Marsden Hospital, Institute of Cancer Research, The Royal Marsden Cancer Charity, the Office of Life Sciences, the UK Medical Research Council, Ventana Medical Systems Inc., Melanoma Research Alliance, and the US Department of Defense during the conduct of the study as well as personal fees from MSD, Roche, AstraZeneca, Novartis, and Ipsen outside the submitted work. No disclosures were reported by the other authors.

Authors' Contributions

R. Culliford: Formal analysis, visualization, writing–original draft. **C. Mills:** Formal analysis, visualization, writing–original draft. **D. Chubb:** Data curation, writing–review and editing. **B. Kinnersley:** Formal analysis, writing–review and editing. **A. Sud:** Formal analysis, writing–review and editing. **A.J. Cornish:** Data curation, formal analysis, writing–review and editing. **L. Browning:** Data curation, writing–review and editing. **S.E. D. Lawrence:** Formal analysis, writing–review and editing. **R. Bentham:** Data curation, formal analysis, writing–review and editing. **A. Frangou:** Formal analysis, writing–review and editing. **A.J. Gruber:** Formal analysis, writing–review and editing. **K. Litchfield:** Data curation, writing–review and editing. **D.C. Wedge:** Formal analysis, writing–review and editing. **J. Larkin:** Data curation, writing–review and editing. **S. Turajlic:** Conceptualization, supervision, funding acquisition, writing–review and editing. **R.S. Houlston:** Conceptualization, supervision, funding acquisition, writing–original draft, project administration.

Acknowledgments

R.S. Houlston acknowledges grant support from Cancer Research UK (C1298/A8362), the Wellcome Trust (214388), and the Medical Research Council. L. Browning received grant support from the National Institute for Health Research (NIHR) Oxford Health BRC (Molecular Diagnostics Theme). S. Turajlic is funded by Cancer Research UK (A29911); the Francis Crick Institute, which receives its core funding from Cancer Research UK (FC10988), the UK Medical Research Council (FC10988), and the Wellcome Trust (FC10988); the NIHR Biomedical Research Centre at the Royal Marsden Hospital and Institute of Cancer Research (grant reference number A109); the Royal Marsden Cancer Charity; The Rosetrees Trust (reference A2204); Ventana Medical Systems Inc (references 10467 and 10530); the NIH (U01 CA247439); Melanoma Research Alliance (reference 686061); the US Department of Defense (award W81XWH-22-1-0652); and VHL Alliance. This research was made possible through access to data in the National Genomic Research Library, which is managed by Genomics England Limited (a wholly owned company of the Department of Health and Social Care). The National Genomic Research Library holds data provided by patients and collected by the NHS as part of their care and data collected as part of their participation in research. The National Genomic Research Library is funded by the NIHR and NHS England. The Wellcome Trust, Cancer Research UK, and the Medical Research Council have also funded research infrastructure.

Note

Supplementary data for this article are available at Molecular Cancer Research Online (http://mcr.aacrjournals.org/).

Received June 10, 2025; revised September 2, 2025; accepted January 15, 2026; posted first January 21, 2026.

References

1. Moch H, Amin MB, Berney DM, Compérat EM, Gill AJ, Hartmann A, et al. The 2022 World Health Organization classification of tumours of the urinary system and male genital organs-part A: renal, penile, and testicular tumours. Eur Urol 2022;82:458–68.
2. Meng L, Collier KA, Wang P, Li Z, Monk P, Mortazavi A, et al. Emerging immunotherapy approaches for advanced clear cell renal cell carcinoma. Cells 2023;13:34.
3. Lobo J, Ohashi R, Amin MB, Berney DM, Compérat EM, Cree IA, et al. WHO 2022 landscape of papillary and chromophobe renal cell carcinoma. Histopathology 2022;81:426–38.
4. Cancer Genome Atlas Research Network. Comprehensive molecular characterization of clear cell renal cell carcinoma. Nature 2013;499:43–9.
5. Mitchell TJ, Turajlic S, Rowan A, Nicol D, Farmery JHR, O'Brien T, et al. Timing the landmark events in the evolution of clear cell renal cell cancer: TRACERx renal. Cell 2018;173:611–23.e17.
6. Culliford R, Lawrence SED, Mills C, Tippu Z, Chubb D, Cornish AJ, et al. Whole genome sequencing refines stratification and therapy of patients with clear cell renal cell carcinoma. Nat Commun 2024;15:5935.
7. Ricketts CJ, De Cubas AA, Fan H, Smith CC, Lang M, Reznik E, et al. The cancer genome Atlas comprehensive molecular characterization of renal cell carcinoma. Cell Rep 2018;23:313–26.e5.
8. Genomics England. The National Genomic Research Library v5.1. 2020. 2020/05/21; Available from: http://dx.doi.org/10.6084/m9.figshare.4530893.v7.
9. Turnbull C. Introducing whole-genome sequencing into routine cancer care: the Genomics England 100 000 Genomes Project. Ann Oncol 2018;29:784–7.
10. Moch H, Cubilla AL, Humphrey PA, Reuter VE, Ulbright TM. The 2016 WHO classification of tumours of the urinary system and male genital organs—part A: renal, penile, and testicular tumours. Eur Urol 2016;70:93–105.
11. Trpkov K, Hes O, Williamson SR, Adeniran AJ, Agaimy A, Alaghehbandan R, et al. New developments in existing WHO entities and evolving molecular concepts: the Genitourinary Pathology Society (GUPS) update on renal neoplasia. Mod Pathol 2021;34:1392–424.
12. Van Loo P, Nordgard SH, Lingjærde OC, Russnes HG, Rye IH, Sun W, et al. Allele-specific copy number analysis of tumors. Proc Natl Acad Sci U S A 2010;107:16910–5.
13. Nik-Zainal S, Van Loo P, Wedge DC, Alexandrov LB, Greenman CD, Lau KW, et al. The life history of 21 breast cancers. Cell 2012;149:994–1007.
14. Martínez-Jiménez F, Muiños F, Sentís I, Deu-Pons J, Reyes-Salazar I, Arnedo-Pac C, et al. A compendium of mutational cancer driver genes. Nat Rev Cancer 2020;20:555–72.

15. Mularoni L, Sabarinathan R, Deu-Pons J, Gonzalez-Perez A, López-Bigas N. OncodriveFML: a general framework to identify coding and non-coding regions with cancer driver mutations. Genome Biol 2016;17:128.
16. Zhu H, Uusküla-Reimand L, Isaev K, Wadi L, Alizada A, Shuai S, et al. Candidate cancer driver mutations in distal regulatory elements and long-range chromatin interaction networks. Mol Cell 2020;77:1307–21.e10.
17. Martincorena I, Raine KM, Gerstung M, Dawson KJ, Haase K, Van Loo P, et al. Universal patterns of selection in cancer and somatic tissues. Cell 2018;173:1823.
18. Paczkowska M, Barenboim J, Sintupisut N, Fox NS, Zhu H, Abd-Rabbo D, et al. Integrative pathway enrichment analysis of multivariate omics data. Nat Commun 2020;11:735.
19. Liberzon A, Birger C, Thorvaldsdóttir H, Ghandi M, Mesirov JP, Tamayo P. The Molecular Signatures Database (MSigDB) hallmark gene set collection. Cell Syst 2015;1:417–25.
20. Gerstung M, Jolly C, Leshchiner I, Dentro SC, Gonzalez S, Rosebrock D, et al. The evolutionary history of 2,658 cancers. Nature 2020;578:122–8.
21. Mermel CH, Schumacher SE, Hill B, Meyerson ML, Beroukhim R, Getz G. GISTIC2.0 facilitates sensitive and confident localization of the targets of focal somatic copy-number alteration in human cancers. Genome Biol 2011;12:R41.
22. Li Y, Roberts ND, Wala JA, Shapira O, Schumacher SE, Kumar K, et al. Patterns of somatic structural variation in human cancer genomes. Nature 2020;578:112–21.
23. Glodzik D, Morganella S, Davies H, Simpson PT, Li Y, Zou X, et al. A somatic-mutational process recurrently duplicates germline susceptibility loci and tissue-specific super-enhancers in breast cancers. Nat Genet 2017;49:341–8.
24. Deshpande V, Luebeck J, Nguyen N-PD, Bakhtiari M, Turner KM, Schwab R, et al. Exploring the landscape of focal amplifications in cancer using AmpliconArchitect. Nat Commun 2019;10:392.
25. Farmery JHR, Smith ML; NIHR BioResource - Rare Diseases; Lynch AG. Telomerecat: a ploidy-agnostic method for estimating telomere length from whole genome sequencing data. Sci Rep 2018;8:1300.
26. Tate JG, Bamford S, Jubb HC, Sondka Z, Beare DM, Bindal N, et al. COSMIC: the catalogue of somatic mutations in cancer. Nucleic Acids Res 2019;47:D941–7.
27. Islam SMA, Díaz-Gay M, Wu Y, Barnes M, Vangara R, Bergstrom EN, et al. Uncovering novel mutational signatures by extraction with SigProfilerExtractor. Cell Genom 2022;2:100179.
28. Salipante SJ, Scroggins SM, Hampel HL, Turner EH, Pritchard CC. Microsatellite instability detection by next generation sequencing. Clin Chem 2014;60:1192–9.
29. Davies H, Glodzik D, Morganella S, Yates LR, Staaf J, Zou X, et al. HRDetect is a predictor of BRCA1 and BRCA2 deficiency based on mutational signatures. Nat Med 2017;23:517–25.
30. Shukla SA, Rooney MS, Rajasagi M, Tiao G, Dixon PM, Lawrence MS, et al. Comprehensive analysis of cancer-associated somatic mutations in class I HLA genes. Nat Biotechnol 2015;33:1152–8.
31. Hundal J, Carreno BM, Petti AA, Linette GP, Griffith OL, Mardis ER, et al. pVAC-Seq: a genome-guided in silico approach to identifying tumor neoantigens. Genome Med 2016;8:11.
32. Bentham R, Litchfield K, Watkins TBK, Lim EL, Rosenthal R, Martínez-Ruiz C, et al. Using DNA sequencing data to quantify T cell fraction and therapy response. Nature 2021;597:555–60.
33. Dawsey SJ, Gupta S. Hereditary renal cell carcinoma. Kidney Cancer 2022;6:83–93.
34. Ohashi R, Schraml P, Angori S, Batavia AA, Rupp NJ, Ohe C, et al. Classic chromophobe renal cell carcinoma incur a larger number of chromosomal losses than seen in the eosinophilic subtype. Cancers 2019;11:1492.
35. Bielski CM, Zehir A, Penson AV, Donoghue MTA, Chatila W, Armenia J, et al. Genome doubling shapes the evolution and prognosis of advanced cancers. Nat Genet 2018;50:1189–95.
36. Bailey C, Pich O, Thol K, Watkins TBK, Luebeck J, Rowan A, et al. Origins and impact of extrachromosomal DNA. Nature 2024;635:193–200.
37. Davis CF, Ricketts CJ, Wang M, Yang L, Cherniack AD, Shen H, et al. The somatic genomic landscape of chromophobe renal cell carcinoma. Cancer Cell 2014;26:319–30.
38. Cancer Genome Atlas Research Network; Linehan WM, Spellman PT, Ricketts CJ, Creighton CJ, Fei SS, DavisC, et al. Comprehensive molecular characterization of papillary renal-cell carcinoma. N Engl J Med 2016;374:135–45.
39. Wang K, Liu T, Liu L, Liu J, Liu C, Wang C, et al. TERT promoter mutations in renal cell carcinomas and upper tract urothelial carcinomas. Oncotarget 2014;5:1829–36.
40. Rathmell KW, Chen F, Creighton CJ. Genomics of chromophobe renal cell carcinoma: implications from a rare tumor for pan-cancer studies. Oncoscience 2015;2:81–90.
41. Gupta S, Vanderbilt CM, Lin Y-T, Benhamida JK, Jungbluth AA, Rana S, et al. A pan-cancer study of somatic TERT promoter mutations and amplification in 30,773 tumors profiled by clinical genomic sequencing. J Mol Diagn 2021;23:253–63.
42. Bailey MH, Tokheim C, Porta-Pardo E, Sengupta S, Bertrand D, Weerasinghe A, et al. Comprehensive characterization of cancer driver genes and mutations. Cell 2018;173:371–85.e18.
43. Yuan Y, Ju YS, Kim Y, Li J, Wang Y, Yoon CJ, et al. Comprehensive molecular characterization of mitochondrial genomes in human cancers. Nat Genet 2020;52:342–52.
44. Chakravarty D, Gao J, Phillips SM, Kundra R, Zhang H, Wang J, et al. OncoKB: a precision oncology knowledge base. JCO Precis Oncol 2017;2017:PO.17.00011.
45. Kroiss M, Reuss M, Kühner D, Johanssen S, Beyer M, Zink M, et al. Sunitinib inhibits cell proliferation and alters steroidogenesis by down-regulation of HSD3B2 in adrenocortical carcinoma cells. Front Endocrinol 2011;2:27.
46. Liu YJ, Ussakli C, Antic T, Liu Y, Wu Y, True L, et al. Sporadic oncocytic tumors with features intermediate between oncocytoma and chromophobe renal cell carcinoma: comprehensive clinicopathological and genomic profiling. Hum Pathol 2020;104:18–29.
47. Choueiri TK, Motzer RJ. Systemic therapy for metastatic renal-cell carcinoma. N Engl J Med 2017;376:354–66.
48. Msaouel P, Genovese G, Tannir NM. Renal cell carcinoma of variant histology: biology and therapies. Hematol Oncol Clin North Am 2023;37:977–92.
49. Wang C, Tan JYM, Chitkara N, Bhatt S. TP53 mutation-mediated immune evasion in cancer: mechanisms and therapeutic implications. Cancers 2024;16:3069.
50. Bergmann L, Albiges L, Ahrens M, Gross-Goupil M, Boleti E, Gravis G, et al. Prospective randomized phase-II trial of ipilimumab/nivolumab versus standard of care in non-clear cell renal cell cancer - results of the SUNNIFORECAST trial. Ann Oncol 2025;36:796–806.
51. Massari F, Mollica V, Fiala O, De Giorgi U, Kucharz J, Vitale MG, et al. Papillary renal cell carcinoma: outcomes for patients receiving first-line immune-based combinations or tyrosine kinase inhibitors from the ARON-1 study. Eur Urol Oncol 2024;7:1123–31.
52. Koshkin VS, Barata PC, Zhang T, George DJ, Atkins MB, Kelly WJ, et al. Clinical activity of nivolumab in patients with non-clear cell renal cell carcinoma. J Immunother Cancer 2018;6:9.
53. McDermott DF, Lee J-L, Ziobro M, Suarez C, Langiewicz P, Matveev VB, et al. Open-label, single-arm, phase II study of pembrolizumab monotherapy as first-line therapy in patients with advanced non-clear cell renal cell carcinoma. J Clin Oncol 2021;39:1029–39.
54. Ciccarese C, Brunelli M, Montironi R, Fiorentino M, Iacovelli R, Heng D, et al. The prospect of precision therapy for renal cell carcinoma. Cancer Treat Rev 2016;49:37–44.